

COB-2023-0160

**SUPERELASTIC TUBULAR STRUCTURES OF CU-AL-MN SHAPE
MEMORY ALLOY OBTAINED BY INVESTMENT CASTING: A
PRELIMINARY STUDY USING 3D PRINTED ABS MODELS**

Railson de Medeiros Nóbrega Alves

Postgraduate Program in Mechanical Engineering, Federal University of Paraíba, João Pessoa – PB, Brazil
railson.nobrega@gmail.com

Leonardo Feitosa Jordão

Federal University of Campina Grande, Campina Grande – PB, Brazil
leonardofjordao@gmail.com

Rodinei Medeiros Gomes (in memoriam)

Department of Mechanical Engineering, Federal University of Paraíba, João Pessoa – PB, Brazil
rodineix@gmail.com

Danielle Guedes de Lima Cavalcante

Department of Mechanical Engineering, Federal University of Paraíba, João Pessoa – PB, Brazil
danielleguedes02@gmail.com

Carlos José de Araújo

Department of Mechanical Engineering, Federal University of Campina Grande, Campina Grande – PB, Brazil
carlos.jose@professor.ufcg.edu.br

Abstract. Cellular structures have been extensively studied for their structural applications, including impact load damping. However, conventional aluminum-based cellular materials suffer from permanent deformations that cannot be reversed even with heating. To overcome this limitation, advanced engineering materials called Shape Memory Alloys (SMA) have been developed. SMAs are metallic materials capable of withstanding large inelastic deformations that can be recovered through heating or mechanical unloading. Cu-based SMAs are particularly interesting for cellular structures due to their potential for shape memory effect (SME) and superelasticity (SE) in lightweight materials. Thus, this work aims to evaluate the behavior of three arrangements of cellular tubular structures (unitary, triangular, and quadrangular) manufactured from a CuAlMn SMA. The SMA was produced using an induction melting furnace, resulting in two ingots of 200 grams. The tubular parts were obtained from these ingots through an investment casting process using a centrifugal machine. After obtaining the structures, dimensional analysis, thermal properties and mechanical behavior characterizations were performed. The results demonstrated that the manufactured CuAlMn SMA exhibited superelasticity characteristics at room temperature. The investment casting process yielded structures with satisfactory dimensions and effective mechanical behavior under compression, indicating their potential as impact dampers for dissipating mechanical energy.

Keywords: Shape memory alloys; CuAlMn alloys; Tubular Structures; Superelasticity; Investment Casting.

1. INTRODUCTION

Shape Memory Alloys (SMA) are functional metallic materials that exhibit unique thermoelastic characteristics compared to conventional engineering metals. These alloys are characterized by two main behaviors: the Shape Memory Effect (SME) and Superelasticity (SE). Due to these special characteristics, applications have been studied in various fields (Lagoudas, 2008).

The SME is associated with the recovery of an apparently plastic deformation in the lower temperature martensitic phase after the application of mechanical loading-unloading cycle followed by heating, causing the SMA to transition to its higher temperature austenitic phase and recover its residual deformation. On the other hand, SE is associated with a stress-induced transformation, where the SMA, in its austenitic phase during mechanical loading, is capable of developing much larger deformations than conventional metallic materials (Otsuka & Wayman, 1998).

Several studies have been performed on the use of cellular structures made of conventional metals, such as honeycombs (structures in the shape of a honeycomb) (Marcadon, 2012). These structures are widely used in mechanical systems that require enhanced resistance to deformation. In such cases, the superelasticity effect of SMAs is highly

advantageous. Therefore, the use of SMAs in these structures holds great promise, particularly as an alternative to conventional metallic materials.

In the study carried out by Machado et al (2015), tubular cellular structures made of NiTi SMA were fabricated and tested. The results presented were satisfactory in terms of the ability to recover from significant deformations (considering that they were thin-walled tubes, approximately 0.32 mm thick) when subjected to compression tests. Furthermore, Simões & De Araujo (2018) clearly demonstrated the possibility of manufacturing cellular structures from NiTi SMA with two different geometries (circular and hexagonal) using the investment casting process.

In general, NiTi-based SMAs are the most commonly used due to the better mechanical properties and biocompatibility. However, the inherent difficulties in processing NiTi-based alloys and their higher cost necessitate the development of alternative SMAs (Silva, 2014). As an alternative to NiTi-based SMAs, there are copper-based SMAs (CuAlNi, CuAlMn, CuAlBe, CuZnAl, among others), which also exhibit good thermal and mechanical properties similar to those of NiTi, with the advantage of a significantly lower cost.

Santana et al. (2018) demonstrated the possibility of obtaining cellular structures of CuAlMn SMA using the investment casting process, revealing promising results compared to NiTi structures (Simões & De Araujo, 2018).

In this sense, this work aims to fabricate and characterize tubular cellular structures with three arrangements (unit cell, triangular and quadrangular) of a superelastic CuAlMn SMA at room temperature, using the investment casting process.

2. MATERIALS AND METHODS

This section describes the main parts of this work: the fabrication of SMA tubular structures by investment casting and the mechanical characterization, as illustrated in Figure 1.

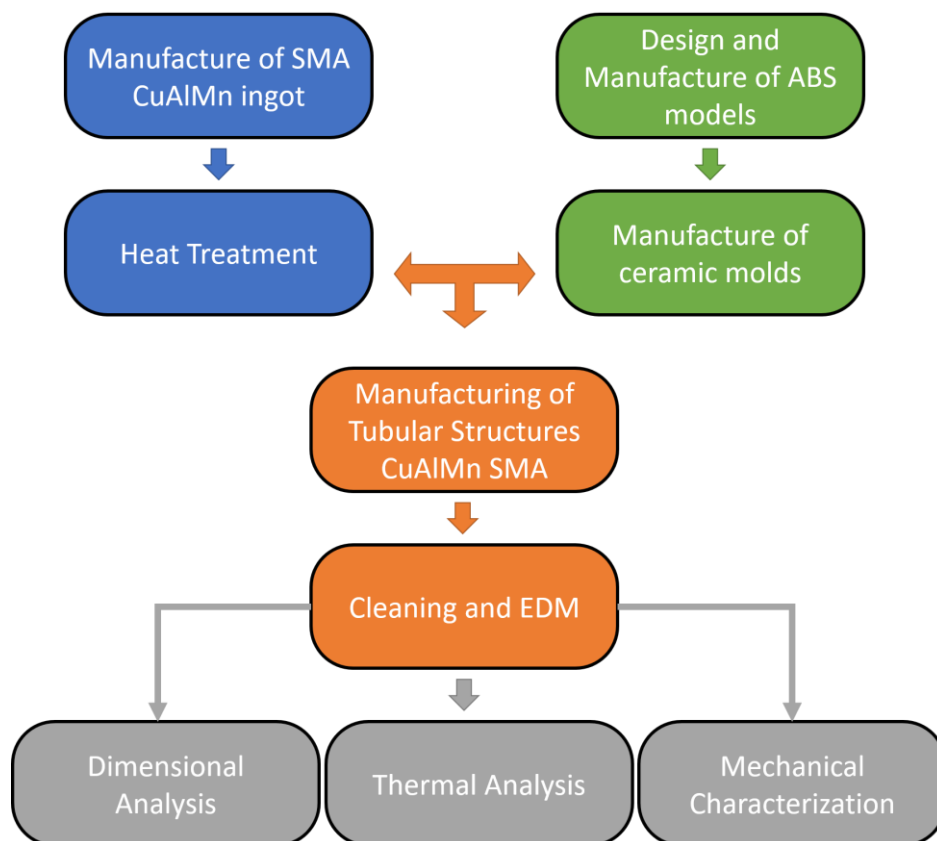


Figure 1. Procedure for the fabrication and mechanical characterization of the CuAlMn SMA tubular structures.

2.1 Manufacture of CuAlMn SMA tubular structures

Initially, the investigation focused on identifying a Cu-based SMA that demonstrated superelasticity properties at room temperature, with the intention of employing it in the production of cellular structures. In this context, an alloy studied by Xu et al. (2017) comprising $\text{Cu}_{80.8}\text{Al}_{8.4}\text{Mn}_{10.8}$ (%wt) was chosen due to its favorable mechanical characteristics and its ability to exhibit superelasticity behavior at room temperature. The induction melting process was performed in a graphite crucible, followed by casting into a rectangular section mold with specific dimensions of 90mm x 30mm x 40mm.

Each ingot was manufactured using approximately 200g of material. Subsequently, the ingots were left to cool in air and subjected to two heat treatments: homogenization at 750°C for 12h followed by furnace cooling, and quenching from 850°C for 30 min in room temperature water.

As illustrated in Figure 2, CAD models were designed based on the geometries proposed by Machado et al. (2015) and printed using ABS (acrylonitrile butadiene styrene) polymer with a MakerBot Replicator 2X 3D printer. Three models were created: one featuring 4 tubes (quadrangular structure), another with 3 tubes (triangular structure), and the last one consisting of a single tube (unitary structure). All ABS models have the same tube dimensions, including an outer diameter of 5.75 mm and a thickness of 0.4 mm, along with a depth of 5 mm (in the z-direction) and 0.4 mm thickness for the base and top walls.

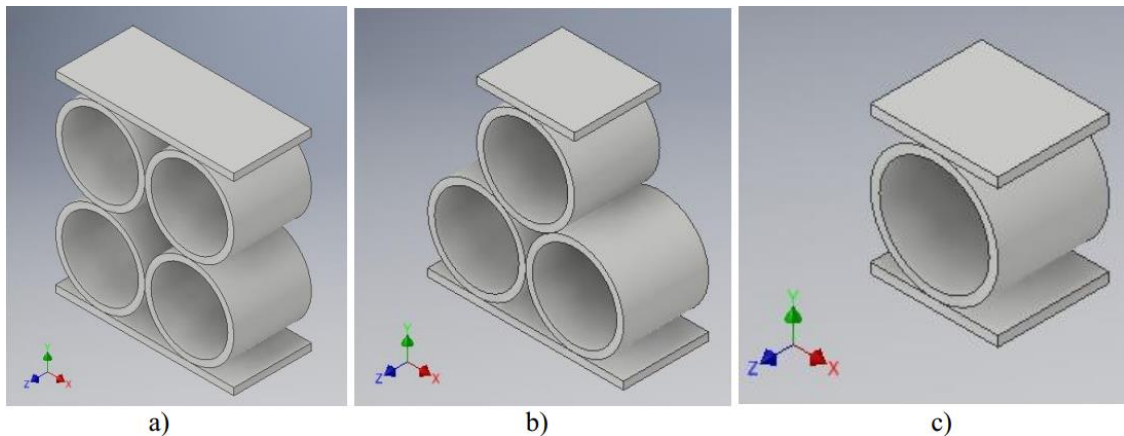


Figure 2. CAD-designed models for ABS 3D printing. a) Quadrangular structure; b) Triangular structure; c) Unitary structure.

To obtain ceramic solid molds of the tree containing the ABS models illustrated in Fig. 2, the Calibra Express ceramic coating (an ultra-thin coating for casting metal alloys) was utilized. Once the coating solidified around the model, the assembly was transferred to an electric furnace and subjected to a heating process. The temperature was increased at a rate of 20°C/min⁻¹ until reaching 750°C, where it was held for a duration of 30 minutes. Subsequently, the ABS polymer was evaporated, resulting in the formation of the desired component's ceramic-coated mold.

For induction melting with centrifugal casting (ICC) process, the Power Cast 1700 - EDG machine was utilized. In this process, the previously prepared CuAlMn SMA is inserted into a ceramic crucible and re-melted using electromagnetic induction, followed by centrifugal injection into the ceramic mold. More details concerning this process can be obtained in the recent work of Albuquerque, Grassi & De Araújo (2023). After cooling to room temperature, the mold is opened to remove the cast tubular structures along with their feeding channels. A preliminary cleaning of the as-cast structure is performed, followed by the removal of the feeding channels using wire electrical discharge machining (EDM) cutting process.

2.2 Characterization of the CuAlMn SMA tubular structures

The characterization of the CuAlMn SMA tubular structures was conducted in the following sequence:

1. Dimensional analyses: this step was performed using optical microscopy (Olympus, BX51 model) to evaluate the precision of the casting process and to estimate the contraction of the SMA tubular structures from the ABS models. The dimensional analysis was conducted on the wall thickness of the tubes and the thickness of the upper and lower support plates of each structure type.

2. Thermal Analysis: the phase transformation temperatures of the SMA tubular structures were analyzed by differential scanning calorimetry (DSC) technique, using a Q20 calorimeter (TA Instruments). Following ASTM standard F2004-05, the tests were carried out between -50°C to 150°C with a heating and cooling rate of 10 °C/min. The average sample mass used in the experiments was approximately 20 mg. The starting and final phase transformation temperatures, both during cooling and heating, were obtained by the tangent intersection method of the DSC peaks.

3. Compression Tests: this step was carried out at room temperature (25°C ± 2°C) using a universal testing machine (Instron, 5582 model). The structures underwent compression at a deformation rate of 0.5%.min⁻¹. Loading-unloading cycles of 1%, 2%, 3%, 6% (unitary and triangular structures), and 9% (quadrangular structure) were performed.

3. RESULTS AND DISCUSSIONS

3.1 Manufacture of tubular structures

After the manufacturing process and cleaning of the parts, the result is the CuAlMn tubular structures in their three geometries. Despite the small thicknesses, the structures exhibited a satisfactory final geometry, as shown in Figure 3.

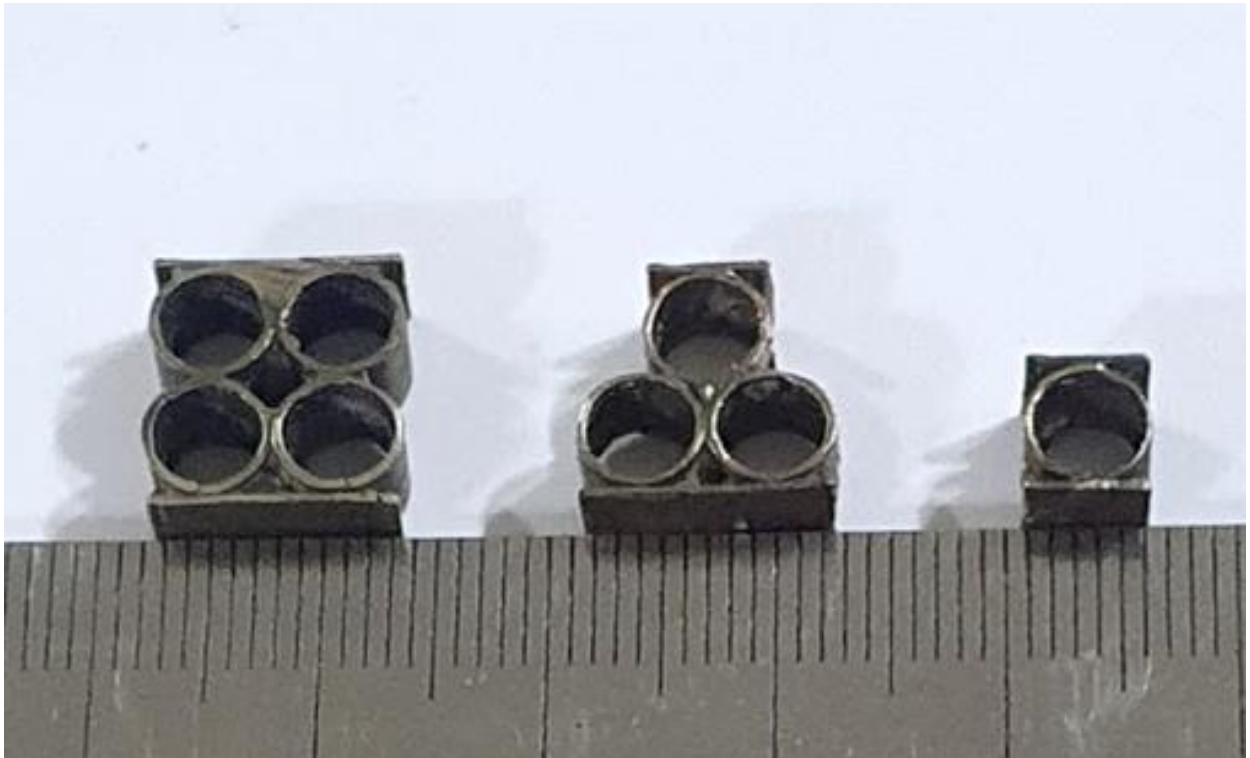


Figure 3. CuAlMn SMA tubular structures obtained by the centrifugal investment casting.

3.2 Dimensional analysis

To compare the resulting printed ABS and CuAlMn SMA models tubular structures, the tube thickness was measured as indicated in Figure 4. The estimated dimensional variation between the ABS models and as-cast obtained parts is presented in Table 1, where the percentage reductions are presented in relation to the ABS models. For this purpose, 10 measurements were taken for each thickness (tube and plate) at different locations.

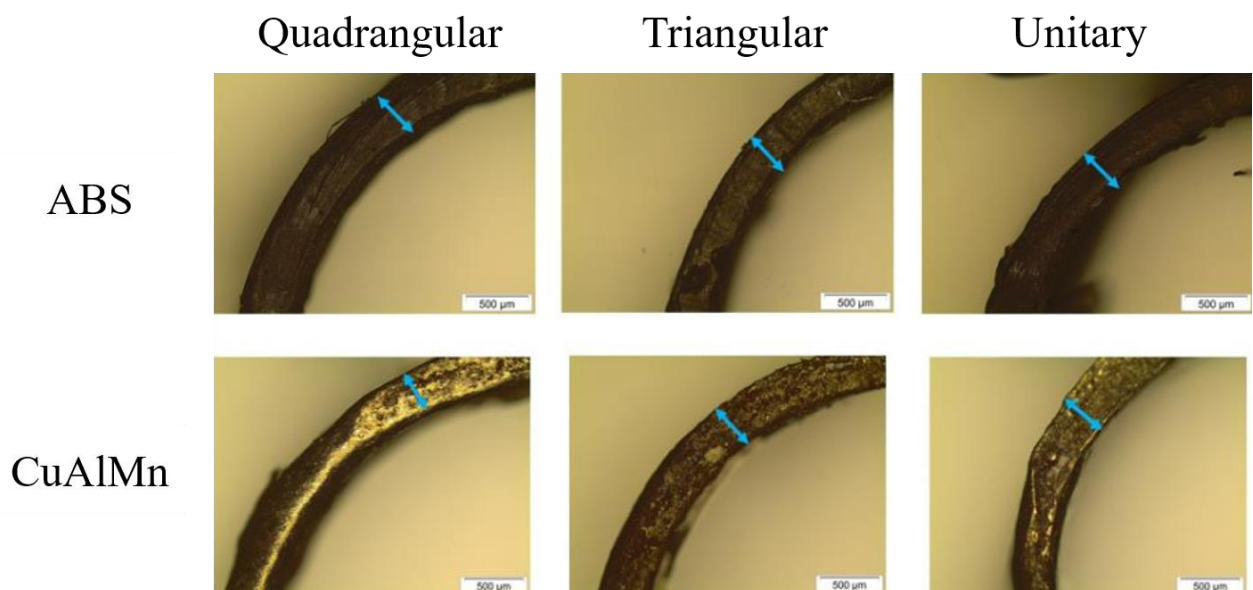


Figure 4. Dimensional evaluation of the ABS models and CuAlMn tubular structures (50x magnification).

The results in Tables 1 and 2 indicate a shrinkage between 2% and 10% in the CuAlMn SMA on the wall thickness of the tubes of each structure type and from the ABS models.

Table 1. Comparisons of the measurements obtained for the tube thickness.

Geometry	Quadrangular	Triangular	Unitary
ABS (mm)	0.394 ± 0.035	0.405 ± 0.034	0.394 ± 0.021
CuAlMn (mm)	0.386 ± 0,016	0.378 ± 0.017	0.377 ± 0.020
Percentage Reductions (%)	2.03	6.67	4.30

Table 2. Comparisons of the measurements obtained for the thickness of the lower/upper plates.

Geometry	Quadrangular	Triangular	Unitary
ABS (mm)	0,398 ± 0,012	0,397 ± 0,009	0,403 ± 0,014
CuAlMn (mm)	0,380 ± 0,026	0,377 ± 0,014	0,363 ± 0,029
Percentage Reductions (%)	4,52%	5,04	9,92

As stated by Sabau (2006), the observed shrinkage is a typical occurrence in the investment casting processes and can be attributed to multiple factors, including solidification, heat transfer, stress distribution, and subsequent deformation behavior of the metal in both the semi-solid and solid states.

A similar behavior was observed in a study realized by Santana et al. (2018), where a shrinkage of 8.9% was observed for wall thicknesses of 0.7 mm. The materials analyzed in the dimensional analyses were ABS and CuAlMn SMA. Alves (2019) demonstrates that as the thickness to be analyzed increases, the metal experiences greater contraction during solidification. However, in terms of the overall height of the cellular structure, the contraction remains below 2.1%, thereby not significantly affecting the final dimensions of the CuAlMn SMA components.

3.3 Thermal Analysis

Figure 5 shown the DSC curves of the samples taken from the tubular structures. From these curves, it was possible to determine the indicated values of transformation temperatures.

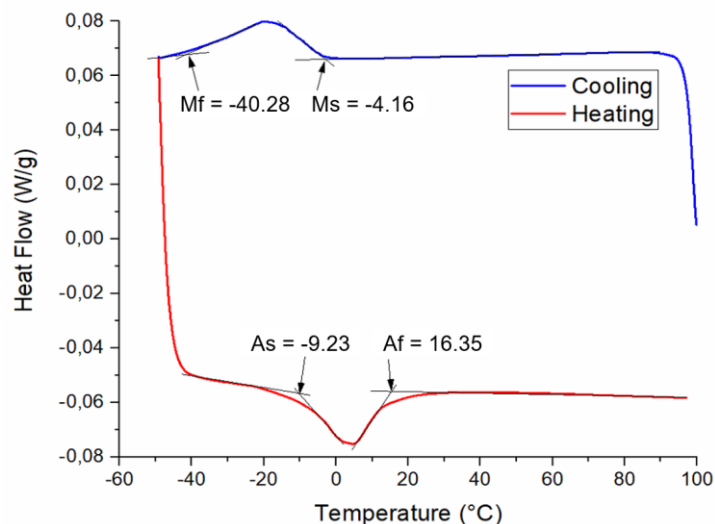


Figure 5. DSC thermal analyses and transformation temperatures of the CuAlMn SMA.

It can be observed that all structures exhibited phase transformation, indicating the potential for superelasticity when subjected to deformations at room temperature (approximately 25 °C). It is important to note that all tubular structures were obtained from the same casting, thus the transformation temperatures are the same.

In the study carried out by Xu et al. (2017), the A_f temperature was -39.6°C . The observed difference in relation to our work can be attributed to some modifications in the chemical composition of the remelted material, as even small changes in composition can result in such variations. Manganese is a highly reactive metal, and a reduction in its percentage, even if minimal, can lead to significant variations in transformation temperatures.

To analyze the chemical composition of the as-cast ingots of the CuAlMn SMA, an Energy Dispersive Spectroscopy (EDS) test was performed. The EDS results obtained can be seen in Table 3.

Table 3. The weight composition of CuAlMn SMA evaluated by EDS.

Composition	Cu	Al	Mn
Nominal (wt%)	80.8	8.4	10.8
As-cast ingot (wt%)	79.9	8.2	11.9

As noted by Zak et al. (1996), even small variations in the chemical composition of CuAlMn SMA can lead to significant changes in the phase transformation temperatures. However, despite the slight variation in the manganese percentage, the CuAlMn SMA retained its superelastic behavior at room temperature.

3.4 Mechanical tests

Following the loading-unloading ramps described in Section 2.2, static compression tests were performed on each of the three structures, as presented in Figure 6.

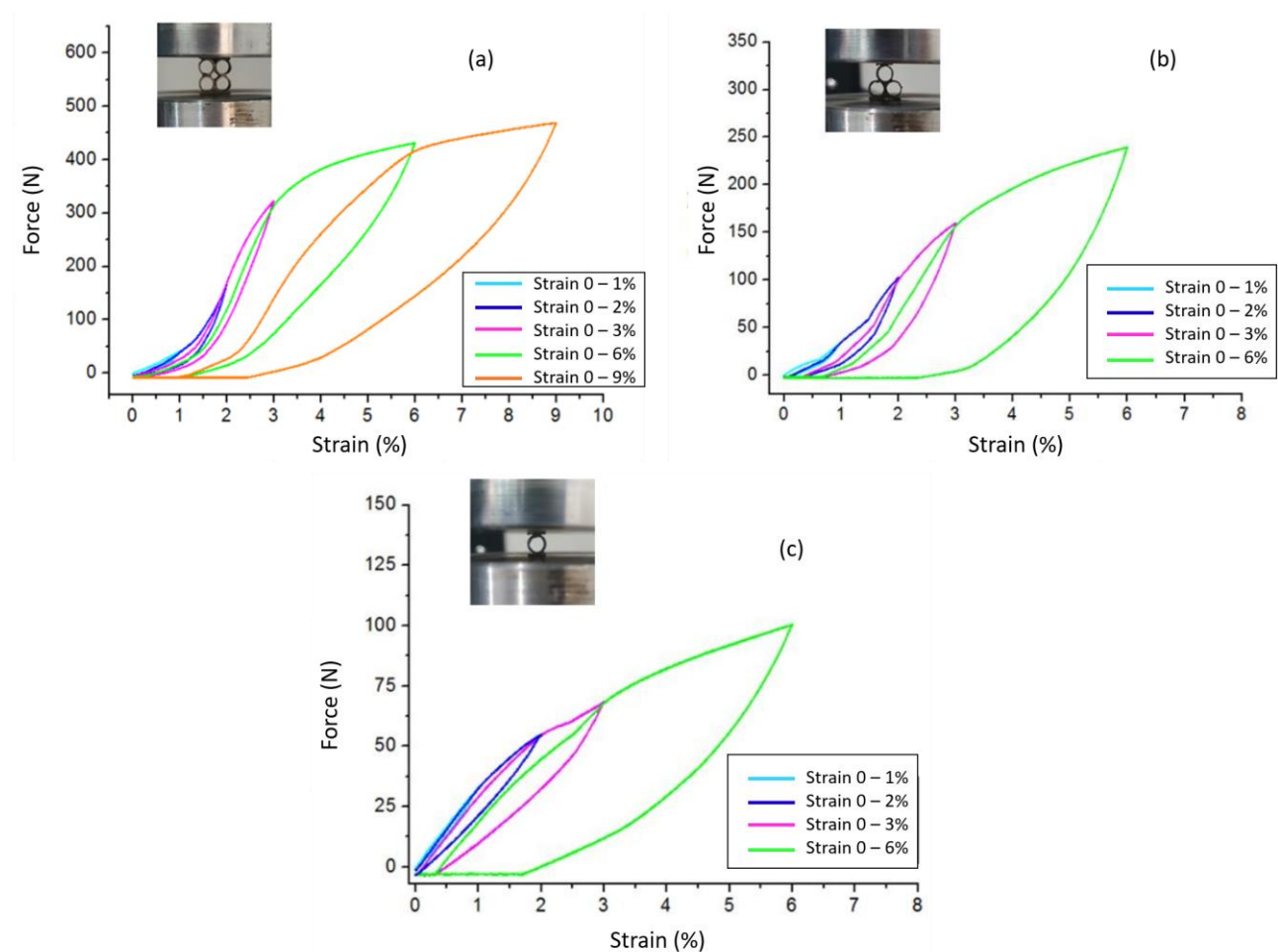


Figure 6. Force vs. Deformation behavior of the tubular structures under compression. a) Quadrangular structure; b) Triangular structure; c) Unitary structure.

In the quadrangular geometry, showed in Figure 7, a good dissipation of mechanical energy can be observed, indicated by the formation of the characteristic superelastic mechanical hysteresis loop, with small residual deformations (<0.5%) up to a deformation limited to 3%. After this point, an increase in residual deformation is observed after unloading, resulting from deformations above 6% and reaching up to 9%, which still remains below 3%.

In the other two geometries, due to the arrangement of the tubes, the force is concentrated mainly on one tube, as can be observed more clearly in Figures 8 and 9. As a result, there is a reduction in the dissipation of mechanical energy in these geometries. Additionally, an important residual deformation is already observed at the deformation level of 6%. In contrast, in the quadrangular geometry, the dissipated energy during the test is more evenly distributed due to the allocation of the tubes, as shown in Figure 7, leading to better results compared to the other geometries.

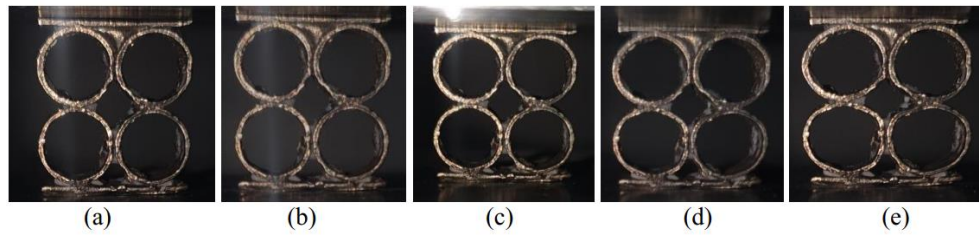


Figure 7. Quadrangular geometry during mechanical testing. a) Undeformed initial configuration; b) Deformation = 1%; c) Deformation = 3%; d) Deformation = 6%; e) Deformation = 9%.

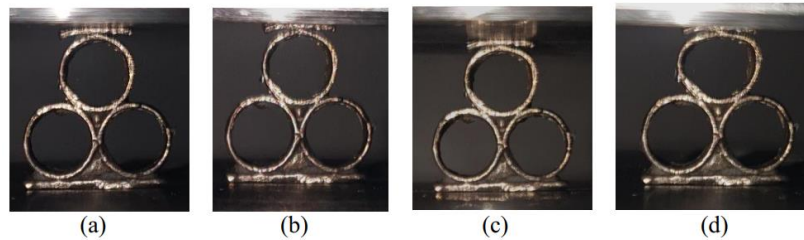


Figure 8. Triangular geometry during mechanical testing. a) Undeformed initial configuration; b) Deformation = 1%; c) Deformation = 3%; d) Deformation = 6%.

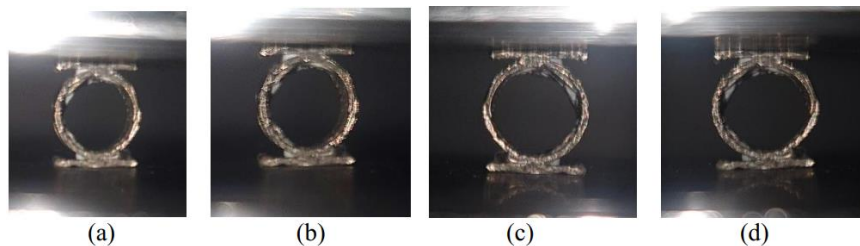


Figure 9. Unitary geometry during mechanical testing. a) Undeformed initial configuration; b) Deformation = 1%; c) Deformation = 3%; d) Deformation = 6%.

Another noteworthy observation is the similarity in behavior found in the study conducted by Alves (2016) on tubular structures made of NiTi SMA. In that study, the quadrangular-shaped structure demonstrated a greater ability to withstand higher deformations compared to the other two structures fabricated by the aforementioned author. However, when compared to the CuAlMn structures, it is evident that the latter exhibited significantly superior performance in terms of deformations. The CuAlMn structures achieved a maximum deformation value of 9%, whereas the NiTi structures reached a maximum of only 3%.

4. CONCLUSIONS

The fabrication of tubular structures through a centrifugal investment casting process using 3D printed ABS models was successfully achieved.

The dimensional variations between the ABS models and the CuAlMn SMA structures were minimal (between 2 and 6% of the thickness), resulting in final parts with dimensions (diameter 5.75 mm and thickness 0.4 mm) very close to the intended design, therefore does not negatively impact component performance.

The fabricated CuAlMn SMA structures exhibited superelasticity characteristics at room temperature, with a final austenitic transformation temperature of approximately 16.35°C.

Mechanical compression tests demonstrated that the CuAlMn tubular structures presented good mechanical energy dissipation (between 100 and 450N, depending on the structure), with the quadrangular geometry presenting more satisfactory results, reaching 9% deformation, while the other two reached 6%.

5. ACKNOWLEDGMENTS

The authors are grateful to Brazilian National Council for Scientific and Technological Development (CNPq) for the scholarship PQ-1C, grant number 302740/2018-0; the Paraíba State Research Support Foundation (FAPESQ-PB) for the

project NISMArt, grant number 044/2023; and the CNPq for the doctoral scholarship to Railson de Medeiros Nóbrega Alves.

6. REFERENCES

- Alves, R. M. N., *Fabricação e caracterização de estruturas tubulares de liga com memória de forma Ni-Ti (Trabalho de Conclusão de Curso – UFCG/CCT) – Campina Grande*, 2016.
- Alves, R. de M. N. Thermomechanical characterization of Cu-Al-Mn shape memory alloy cellular structures obtained by investment casting. 100 pages. 2019. Master - Postgraduate Program in Mechanical Engineering, Federal University of Campina Grande, Campina Grande, PB, 2019.
- da Silva Albuquerque, C.E., Grassi, E.N.D. & De Araújo, C.J. Castability of Cu-Al-Mn shape memory alloy in a rapid investment casting process: computational and experimental analysis. *Int J Adv Manuf Technol* 127, 2563–2579 (2023).
- de Brito Simões J, de Araújo CJ. Nickel–titanium shape memory alloy mechanical components produced by investment casting. *Journal of Intelligent Material Systems and Structures*. 2018;
- Lagoudas, D. *Shape Memory Alloys: Modeling and Engineering Applications*, Editora: Springer Science+Business Media, LLC, 2008.
- Machado, G. et al., Superelastic cellular NiTi tube-based materials: Fabrication, experiments and modeling. *Materials & Design*, Vol. 65, pp. 212–220, 2015.
- Marcadon, V. Mechanical behaviour of hollow-tube stackings: Experimental characterization and modelling of the role of their constitutive material behaviour. Onera – The French Aerospace Lab, Chatillon, France. 2012.
- Otsuka, K e Wayman, C.M. *Shape Memory Materials*, Cambridge University Press, Cambridge UK. p.1-131. 1998.
- Sabau A S. Alloy shrinkage factors for the investment casting process. *Metallurgical and Materials Transactions B*, v. 37, p. 131-140, 2006.
- Santana, Y. N. de L.; Da Silva, P. C. S.; Calazans, R. N. D.; De Araújo, C. J. *Fabricação de Honeycombs de Liga com Memória de Forma Cu-Al-Mn usando fundição de precisão. X Congresso Nacional de Engenharia Mecânica (CONEM)*, Salvador, p. 1-7, 2018.
- Silva, J. A. S., *Estudo das propriedades termomecânicas de ligas Cu-Al-Mn com memória de forma (Dissertação de Mestrado – UFPB/CT) – João Pessoa*, 2014.
- Xu, S.; Huang H.; Xie J.; Kimura, Y.; Xu, X.; Otori, T.; Kainuma, R. Dynamic Recovery and Superelasticity of Columnar-Grained Cu–Al–Mn Shape Memory Alloy. *Metals*, [s.l.], v. 7, n. 4, p.141-149, 15 abr. 2017.
- Zak, G., Kneissl, A. C., Jatulskij G. Shape memory effect in cryogenic Cu-Al-Mn alloys. *Scripta materialia*, v. 34, n. 3, 1996.

7. RESPONSIBILITY NOTICE

The authors are the only responsible for the printed material included in this paper.